Analyzing Angle-Gather Spectograms: Going Beyond Seismic Resolution

Karimzadanzabi, A.; Cuesta Cano, A.; Verschuur, E.

DOI
10.3997/2214-4609.202410931

Publication date
2024

Document Version
Final published version

Citation (APA)
Karimzadanzabi, A., Cuesta Cano, A., & Verschuur, E. (2024). *Analyzing Angle-Gather Spectograms: Going Beyond Seismic Resolution*. Paper presented at 85th EAGE Annual Conference & Exhibition 2024, Oslo, Lillestrøm, Norway. https://doi.org/10.3997/2214-4609.202410931

Analyzing Angle-Gather Spectograms: Going Beyond Seismic Resolution

A. Karimzadanzabi[1], A. Cuesta Cano[1], E. Verschuur[1]

[1] TU Delft

Summary

This extended abstract discusses a novel approach to identify geological sub-seismic scale features using angle-gather spectrograms. Traditional seismic methods face challenges in identifying fine scale geological structures, especially in sublayers thinner than about 1/10 of the wavelength. This paper introduces the use of spectrogram analysis on angle gathers, to capture local spectrum information which is not visible and distinguishable in the reflectivity image and angle gathers themselves. The authors apply this technique to simulated seismic data for a range of basic geological scenarios, extracting spectrograms for each incident angle within angle gathers. The analysis explores the impact of density, velocity variations, layer number and layer thickness on spectrogram patterns, providing insights into their effectiveness for computer vision-related research. The study aims to rejuvenate the utilization of spectrograms for revealing hidden geological structures beyond standard seismic resolution.

Analyzing Angle-Gather Spectrograms: Going Beyond Seismic Resolution

Conventional seismic approaches face difficulties in identifying and categorizing fine-scale features in stratigraphic analysis, particularly in sub-layers thinner than $1/10^{th}$ of the wavelength. A thorough understanding of subsurface characteristics is hampered by the limits of conventional imaging methods, such as wavelength limitations and lack of sensitivity to small angle variations (Gisolf and van den Berg, 2010). Aware of these difficulties, scientists are looking at different methods to extract more information from traditional images (Liu and Marfurt, 2007). Using the hidden information within frequency components is one method that goes beyond depending only on temporal/depth data. Due to this, spectrogram analysis - based on a windowed Fourier transformation with a changing center — has become more widely used (Li and Lu (2014); Seuret-Jiménez et al. (2023)). With this technique, the local spectrum of frequencies present in subsurface images is efficiently captured, offering joint time-frequency or depth-frequency information that goes beyond traditional seismic amplitude analysis.

In this paper, we revive the efficacy of spectrograms in revealing hidden structures through a comprehensive analysis. The novelty of this paper is rooted in the extraction of spectrograms for each incident angle within angle gathers. We aim to elucidate the capabilities and limitations of spectrograms, providing insights into their effectiveness in discerning the presence, layer thickness, and lithology of fine-structure layers. Our current analysis employs the finite difference method to generate seismic data for some basic geological scenarios. We, next, expand on our analysis by estimating images within the target region, obtaining angle-dependent data (Davydenko and Verschuur, 2017) and their spectrograms.

This process introduces additional dimensions to the subsurface angle-gather cube. Different geologic scenarios provide different and distinct patterns in these higher-dimensional space. Such data may serve as a fundamental basis for computer vision-related research for target characterization in the future.

Theory of the Gabor spectrogram

The fundamental concept involves presenting a depth-dependent spectrum by applying a Fourier transform to distinct depth segments of the signal. In mathematical terms, the spectrogram S is a function of both depth z and vertical wavenumber k_z and can be defined as follows:

$$S(k_z, z) = \int_{-\infty}^{\infty} m(z')g(z'-z)e^{-ik_z z'}\,dz'$$

Here, $m(z)$ represents the signal under examination (depth domain), while $g(z)$ is a gate function, possibly exhibiting a Gabor filter. The $e^{-jk_z z'}$ is the Fourier kernel. This process is then repeated by shifting the window in z using $g(z'-z)$ (Chakraborty and Okaya, 1995).

Methodology

For this analysis, a set of basic 2D subsurface models is create, featuring single to triple sub-layers with thicknesses ranging from 2 to 20 meters, and varying velocity and density values within the common range of sand, marl, and lime, were utilized to establish a laterally homogeneous medium. These models were designed to mimic simplified versions of coarsening/thinning upward trends observed in geological contexts. Subsequently, an acoustic 2D finite difference method was applied to these target models to generate seismic datasets, also including a simple overburden of some geologic layers. The maximum frequency in the modeling is 75 Hz and with a background velocity of 2800 m/s, we expect a vertical resolution in the best case scenario of about $1/10\lambda$, which is about 4 m.

A target-oriented full wavefield migration (Davydenko and Verschuur, 2017) technique was employed to extract both reflectivity image and angle gathers along the lateral location. While the subsurface image is a 2D gather, the expansion of each target location into an angle gather provides a 3D image cube, such as displayed in Figure 1a for a specific target model. Note that if we sum the information along the angle direction, we get the (wide-angle) depth-image. Note also that the side-planes of this cube (and all other cubes in this paper) represent cross-section through the center of the cube along that direction.

The traditional spectrogram approach transforms the two-dimensional reflectivity image to a three-dimensional cube, where now the depth axis is expanded into a 'frequency' axis, which we will call vertical wavenumber k_z, such as shown Figure 1b. By itself, this can already provide useful additional information on the subsurface image, revealing certain details that are unseen in the image domain itself. In the late 1990's and early 2000's, this was one of the popular methods to extract features or attributes from the seismic images, such as described by Castagna et al. (2003) and Steeghs and Drijkoningen (2001).

However, in prior research, spectrograms were not applied to angle gathers, and the influence of the amplitude versus angle (AVA) effect on spectrograms was not accounted for. Thus, we can go one step further and calculate the spectrogram for each relfection angle in the angle-gathers. Then the 3D angle-gather cube (Figure 1a becomes as four-dimensional volume. For display purpose we have selected the subset of this 4D volume and we show the result for the zero-angle only in Figure 1c.

In this study, we examine the spectrogram of the angle gathers for the central column (zero angle), as well as those of neighboring columns (zero-, near-, middle-, far-angle spectrogram). We have setup a set of subsurface model with the same overburden and variations in the target area that are all considered to be at the edge of seisimc resolution. Layer thickensses vary between 2m and 20m and there may be single-, double- and triple-layer target models. To keep the number of experiments limited, we only considered repetition of the same layer in case of double- or triple-layer models.

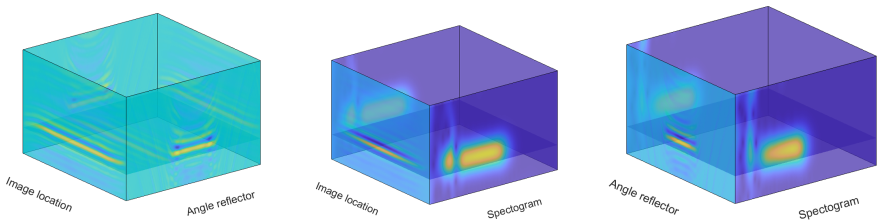

(a) ***(b)*** ***(c)***

Figure 1: *3D represenations of the target area for one basic subsurface model, (a) Reflectivity-angle gather cube, (b) Reflectivity-spectrogram cube,(c) Zero angle-spectrogram cube.*

To better understand the patterns, the current investigation results have been divided into three categories: 1) density and velocity variation effects on spectrogram patterns, 2) effect if different angles on these patterns, and 3) the effect of number of layers and their thickness on these patterns.

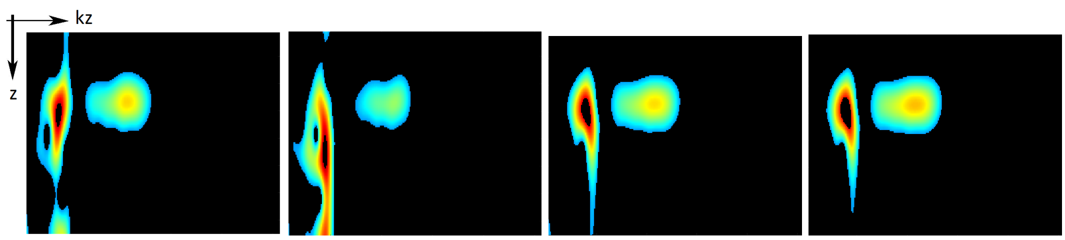

(a) $\Delta v = 0$, $\Delta\rho = 200$. ***(b)*** $\Delta v = 0$, $\Delta\rho = 400$. ***(c)*** $\Delta v = 200$, $\Delta\rho = 0$. ***(d)*** $\Delta v = 400$, $\Delta\rho = 0$.

Figure 2: *Mid-angle gather spectrogram changes for a single layer with thickness 2 meter, the Δv-values are in m/s, the $\Delta\rho$-values in kg/m^3.*

1) Density and velocity variations

Figure 2 illustrates the angle gather spectrogram variations for a solitary 2-meter thin target layer in presence of various density and velocity variations. This figure reveals two distinct blobs for each model. Note that all spectrograms have been normalized on their own maximum amplitude, although the models in Figure 2b and 2d represent stronger reflectivity values compared to the other two. By comparing the spectrograms in Figure 2a and Figure 2b, it shows that density fluctuations have a more pronounced impact on the first, low-frequency pattern compared to velocity variations. Subsequently, by comparing Figure 2c and Figure 2d, the velocity distribution within each layer manifests as a more noticeable influence on the brightness of the second 'anisotropic ellipse' blob. Consequently, density fluctuations primarily impact the low spatial frequency component, while variations in velocity play a role in influencing the higher spatial frequencies.

2) Different angle effects

In our next analysis phase, from the angle gathers, the spectrogram for zero-, near-, mid-, and far-angle are calculated to investigate the effects of amplitude versus angle, as illustrated in Figure 3b to 3e. An examination of the spectrogram for the traces shown in the chosen angle gather (Figure 3a) reveals the presence of two distinct blobs. Moving from zero angle to far angle, the brightness index shifts to the higher frequencies. The first loop which is associated with lower spatial frequencies shows distortion and tends to diminish (From Figure 4a to Figure 4d). The outcomes are compatible with the traces peaks and troughs signature in Figure 3b to Figure 3e. These observed patterns serve as indicators of variations that may hold crucial information not readily apparent in conventional AVO analyses. Uncovering and understanding these variations could be pivotal for extracting hidden information from the seismic data beyond standard seismic resolution.

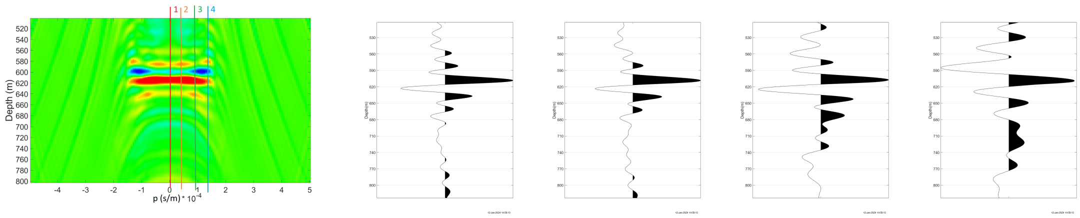

(a) *Central angle gather* ***(b)*** *zero angle (1)* ***(c)*** *near angle (2)* ***(d)*** *mid angle (3)* ***(e)*** *far angle (4)*

Figure 3: *(a) Subsurface angle gather for a single 2-meter thickness target layer obtained after the FWM step for the central location. (b) trace for ray parameter 0, (c,d,e) traces for near-,mid- and far-angle ray pararmeters.*

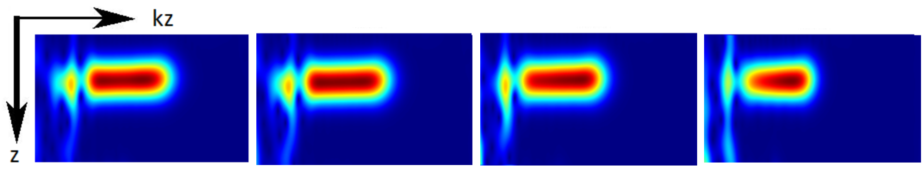

(a) *Location 1 (zero angle).* ***(b)*** *Location 2 (near angle).* ***(c)*** *Location 3 (mid angle).* ***(d)*** *Location 4 (far angle).*

Figure 4: *Spectrogram for different ray-parameter in Figure 3.*

3) Different thickness and number of target layers

In the case of different number and thickness of layers (Figure 5), we start with a model with just a single layer with a two-meter thickness, for which the spectrogram demonstrates two distinct patterns (Figure 5a,5f). By adding another two-meter thickness layer with a two-meter layer separation, the second pattern in the spectrogram distorts for lower k_z values (Figure 5b,5g). If we continue this trend by adding the third layer of two-meter thickness, this distortion shifts toward higher k_z values (Figure 5c,5h). Hence, the layer number manifests itself as a distortion in the spectrograms. It is noteworthy to mention that the number of layers was not distinguishable in the associated angle gather itself, as the 2m thickness is beyond seismic resolution. By increasing the layer thickness rather than the layer abundance, the patterns do not distort but become disconnected. For example, comparing the models for a single layer of 2 meters and a 5-meter target layer with precisely the same density and velocity distribution (Figures 5a, 5f, 5d, and 5i), we observe a shift in patterns towards disconnected configurations for higher k_z values. Additionally, it is evident that when the layer of exact thickness consists of the same velocity distribution (Figure 5d, 5i), it contains fewer k_z values compared to a layer of the same thickness with non-homogeneous velocity and density content.

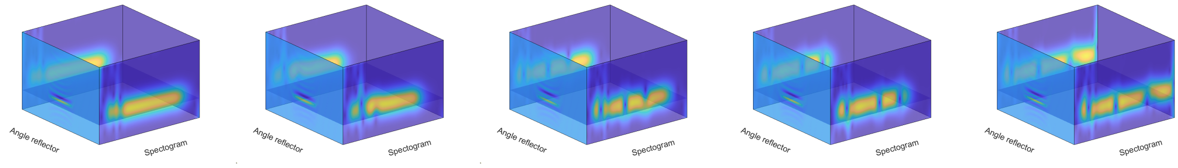

(a) *(b)* *(c)* *(d)* *(e)*

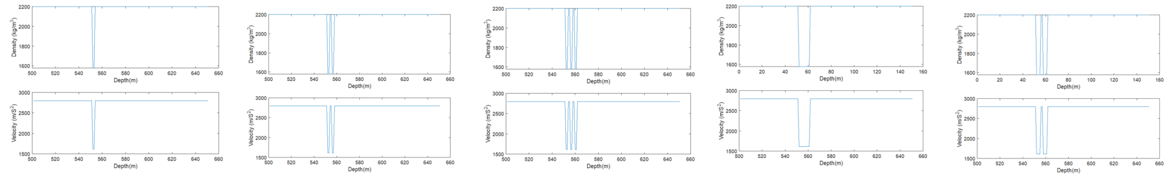

(f) Single-layer target 2 m thickness. *(g) Double-layer target 2 m thickness.* *(h) Triple-layer target 2 m thickness.* *(i) Single-layer target 10 m thickness.* *(j) Double-layer target 4 m thickness.*

Figure 5: *The spectrogram patterns for various target-layer-setting with corresponding density and velocity structure.*

Conclusions

In this paper, our objective is to rejuvenate the utilization of spectrograms in extracting detail from seismic images beyond standard seismic resolution. Specifically, we presented the application of angle-gather spectrograms for the classification of very fine structures that couldn't be classified or detected using conventional seismic methods. Furthermore, we delved into the influences of density and velocity contrasts, the angle of incidence and the thickness and number of these fine layers on the observed patterns. We showcased that each of these factors provides a distinct effect on the spectrogram patterns, rendering them valuable inputs for future computer vision analysis and machine learning applications for recognizing small-scale geologic features.

Acknowledgements

The authors express gratitude to the sponsors of the Delphi consortium for their support.

References

Castagna, J.P., Sun, S. and Siegfried, R.W. [2003] Instantaneous spectral analysis: Detection of low-frequency shadows associated with hydrocarbons. *The Leading Edge*, **22**(2), 120–127.

Chakraborty, A. and Okaya, D. [1995] Frequency-time decomposition of seismic data using wavelet-based methods. *GEOPHYSICS*, **60**(6), 1906–1916.

Davydenko, M. and Verschuur, D. [2017] Full-wavefield estimation of angle-dependent reflectivity and migration velocity. In: *SEG Technical Program Expanded Abstracts 2017*, SEG Technical Program Expanded Abstracts 2017. SEG, 5631–5635.

Gisolf, A. and van den Berg, P. [2010] Target-oriented non-linear inversion of time-lapse seismic data. In: *SEG Technical Program Expanded Abstracts 2010*. 2860–2864.

Li, F. and Lu, W. [2014] Coherence attribute at different spectral scales. *Interpretation*, **2**(1), SA99–SA106.

Liu, J. and Marfurt, K.J. [2007] Instantaneous spectral attributes to detect channels. *GEOPHYSICS*, **72**(2), P23–P31.

Seuret-Jiménez, D., Trutié-Carrero, E., Nieto-Jalil, J.M., García-Aquino, E.D., Díaz-González, L., Carballo-Sigler, L., Quintana-Fuentes, D. and Gaggero-Sager, L.M. [2023] Feature Extraction of a Non-Stationary Seismic–Acoustic Signal Using a High-Resolution Dyadic Spectrogram. 13. 6051.

Steeghs, P. and Drijkoningen, G. [2001] Seismic sequence analysis and attribute extraction using quadratic time-frequency representations. *GEOPHYSICS*, **66**(6), 1947–1959.